A FINITE-ELEMENT INVESTIGATION OF COLLAGEN-FIBRIN CO-GEL MICROSTRUCTURE

A THESIS SUBMITTED TO THE FACULTY OF THE UNIVERSITY OF MINNESOTA BY

DANESH BANKWALA

IN FULFILLMENT OF THE REQUIREMENTS
FOR THE DEGREE OF MASTER OF SCIENCE

ADVISOR: VICTOR H. BAROCAS.

APRIL 2017

Copyright page

Abstract

The mechanics of collagen-fibrin co-gels are useful and scientifically interesting. These proteins, along with elastin, are major components of connective tissue in the human body, and understanding how they interact can help shed light on the mechanics of human tissue. Scaffolds made of these networks are a staple of tissue engineering research. However, the relationship between the properties of the pure components and those of the co-gels has been difficult to specify. Our group has previously found that at high collagen fractions, co-gels behave according to a parallel (solid mixture) model, but fibrin-rich gels exhibit more series-like behavior. This observed phenomenon suggests there is a fundamental change in the way the two components interact as the co-gel's composition changes.

In this study, we explored the hypothesis that this interesting mechanical behavior stems from failure of the dilute component to form a fully percolating network. The hypothesis seemed plausible because a nonpercolating dilute network would only be able to affect the co-gel's behavior with fiber-fiber interactions, which would resemble a series model. To test this hypothesis, we generated a set of computational model networks in which the high-density component percolates the model space but the low-density component does not, instead occupying a small island embedded within the larger network. When the

composite model is stretched, the only stretching the embedded network experiences is due to the crosslinks between the major and minor networks.

When we applied this model to collagen-rich co-gels with embedded fibrin islands, the mechanics of the stiffer collagen gel were largely unaffected by the embedded fibrin gel, leading to parallel behavior at the macroscopic scale, consistent with our hypothesis. However, when a stiff collagen network was embedded in the more compliant fibrin network, the fibrin network's deformation was not markedly altered either. The parallel model exhibited an earlier transition in behavior, but neither model was able to replicate the experimental results. It is likely that the underlying model underestimates how much the proteins interact with each other and that a parallel-like model with much more internetwork fiber interaction would capture the experimentally observed behavior better.

Table of Contents

List of Tables

List of Figures

1. Introduction

Finite Element Modeling (FEM) of the behavior of double networks or interpenetrating fibrous networks (IPNs) has useful applications in many different fields, such as biomechanics, polymer development, textiles, and tissue engineering. In biomechanics, two-component finite element modeling has been used to study abdominal aortic aneurysm (Raghavan & Vorp, 2000). In the field of textiles, FEM of fibrous networks is used to model the bulk properties and draping behavior of different woven or knitted fabrics (Veit, D., 2012). In addition, FEM has been used to study electronic properties of interpenetrating dielectric elastomers (Goulbourne, 2011).

In the field of tissue engineering, our group is particularly interested in biological networks of collagen and fibrin (Lai et al., 2012). As important components of the extracellular matrix (ECM) in soft biological tissues, these proteins can serve as scaffolds for bioartificial tissues (Rao, Peterson, Ceccarelli, Putnam, & Stegemann, 2012; Rowe & Stegemann, 2006). The mechanical properties, and specifically the elastic moduli, must be tailored to each application, because the bulk properties of the scaffold will affect cellular differentiation, growth, migration, and seeding (Heris et al., 2016). Consequently, tissue engineers who work with scaffolds are interested in models for biomimetic networks of proteins such as collagen and fibrin. Understanding how these proteins interact is essential for constructing valid mechanical models of human

tissues. Thus, the mechanical behavior of collagen and fibrin, especially together in a co-gel (a physical gel made from two different proteins) or in models of IPNs (a somewhat idealized model of the co-gel), is important to materials scientists, tissue engineers, and biomechanicists.

In the past, we and others have studied the interaction of these proteins by mixing collagen and fibrin together to fabricate co-gels, then performing uniaxial stretch tests on the resulting gels. While these tests provide a wealth of information about the bulk properties of the gels (elastic modulus, Poisson's ratio, failure strain and failure stress, and stress-strain curves), they are limited in their ability to inform us about the microstructure of these gels and particularly how the proteins interact with each other at the microscopic scale. We have turned to FEM to explore study the way these proteins interact. Unlike physical experiments, FEM allows us to investigate hypotheses about different microstructures and interaction mechanics by comparing those microstructural configurations' macroscopic effects to data from our physical experiments.

Single-component fiber networks can now be modeled by various methods (Hatami-Marbini, Shahsavari, & Picu, 2013; Stylianopoulos & Barocas, 2007) but, as is the case for many composite materials, predicting the properties of a co-gel from those of the individual components is a considerable challenge. In a previous study (Lai et al., 2012), we compared uniaxial tensile tests performed on collagen-fibrin co-gels at various compositions with computational model predictions for parallel (two distinct interpenetrating networks, each made of a

different protein) and series (one continuous network made of fibers randomly assigned as either protein) interactions between the two networks.

In this study, the failure strain of the co-gels decreased smoothly and rapidly from ~ 500% for pure fibrin to ~ 100% for the 40%-collagen gel, but decreased much more slowly to a value of ~ 50% strain as collagen content was increased from 40% to 100% (pure collagen). In the same series of experiments, the ultimate tensile strength of the co-gels was roughly constant at about 5 kPa. The smooth change in failure strain is suggestive of a series model because no parallel collagen component could stretch as much as the fibrin does. However, the experimentally observed behavior seemed to transition from behaving like a series model at low collagen levels to a parallel model at a higher collagen concentration.

In an effort to explain the results with a single model rather than two separate models, we allowed fibers from one network to interact with fibers from the other network. Adding fiber-fiber interaction to the parallel model allowed the two distinct networks to combine. The resulting network looked like an intermediate condition between a parallel double network model and a series single network. Its behavior was closer to the experimentally observed behavior than that of either the series or the noninteracting parallel model, but was still inaccurate enough to suggest that it could not completely explain the mechanics of these co-gels.

Taken together, these observations suggest that the more dilute fiber

network may not be percolating the entire space. Rather, two distinct structures may exist: a continuous network of the denser component, decorated in some areas by clusters of a second, interpenetrating network of the more dilute component. In this study, we tested the hypothesis that the lower density protein forms local, non-percolating regions within the higher density protein network by performing computational simulations with such networks and comparing the results to our previous experimental data. We also wanted to see if the experimentally observed transition from parallel to series behavior could be explained by a change in which protein dominated the co-gel (for the experimental samples) or IPN (for the simulations). Our hypothesis was that when only collagen spanned the box, the IPN would behave mostly like collagen, but when only fibrin spanned the box, the results would reflect the earlier observed transition from series to parallel behavior.

Network structure choice:

Our early work used networks generated by Delaunay triangulation. These networks introduced limitations because the topology of the Delaunay networks was such that the networks consistently failed to capture the behavior of collagen in the toe region of its stress-strain curve. Delaunay networks have high degrees of connectivity, and the high connectivity makes it harder for the nodes to rotate freely. As a result, our Delaunay models were unable to match the slopes (elastic moduli) in both the toe region and the linear region of

collagen's stress-strain curve. The optimization procedure we used to fit the parameters for the Delaunay model minimized the sum of squared errors, which biased the models toward matching in the linear region at the expense of the toe region to minimize error. Figure 1 demonstrates the Delaunay networks' excess stiffness for collagen. The fit is fine for fibrin because fibrin has a much more linear stress-strain curve than collagen does, rather than having a distinctive toe region.

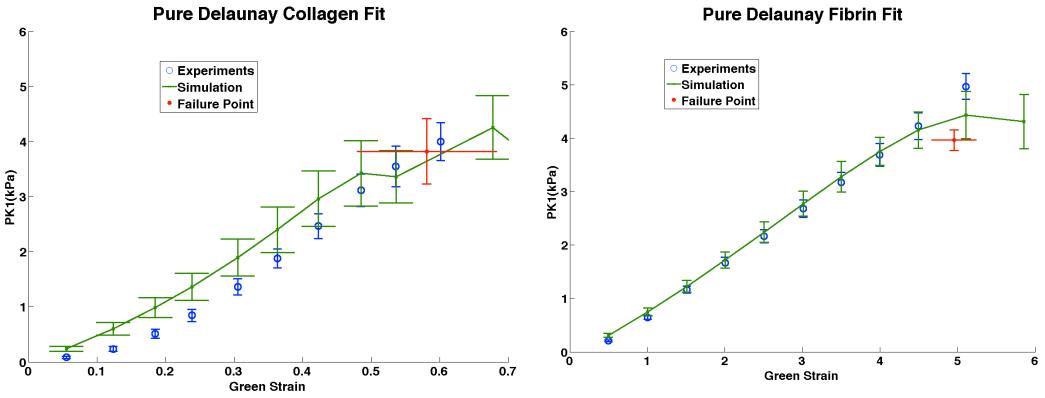

Fig 1a: Best fit of collagen parameters for Delaunay networks. Green Strain is a measure of strain. PK1 is the 1st Piola-Kirchoff stress on the +X face of the network. The simulation behaves more linearly than the physical co-gels, particularly at the start in the toe region, due to Delaunay networks' high connectivity. The collagen fit consistently overshoots collagen's toe region, only achieving a closer fit toward the end. A note on failure: it is not uncommon for the stress in these networks to drop on one step and increase more on subsequent steps.
Fig 1b: Best fit of fibrin parameters for Delaunay networks. Fibrin has a much less pronounced toe region, so the extremely linear behavior of the Delaunay network does not compromise the fit.

We switched to Voronoi tessellation to generate our networks and found the resulting networks fit much better, supporting Nachtrab's finding (2011) that

Voronoi networks approximate collagen well. The fits can be seen in figure 2 and are significantly better for collagen than the Delaunay networks were.

The network type did not display as marked a difference for fibrin, because fibrin's stress-strain curve is much more linear with a less pronounced toe-region. Delaunay networks replicated fibrin's stress-strain curve as well as did the Voronoi networks. However, Voronoi networks reproduced fibrin's failure strain and stress more closely than the Delaunay networks did, making Voronoi tessellation our preferred method for generating fibrin networks in our simulations as well.

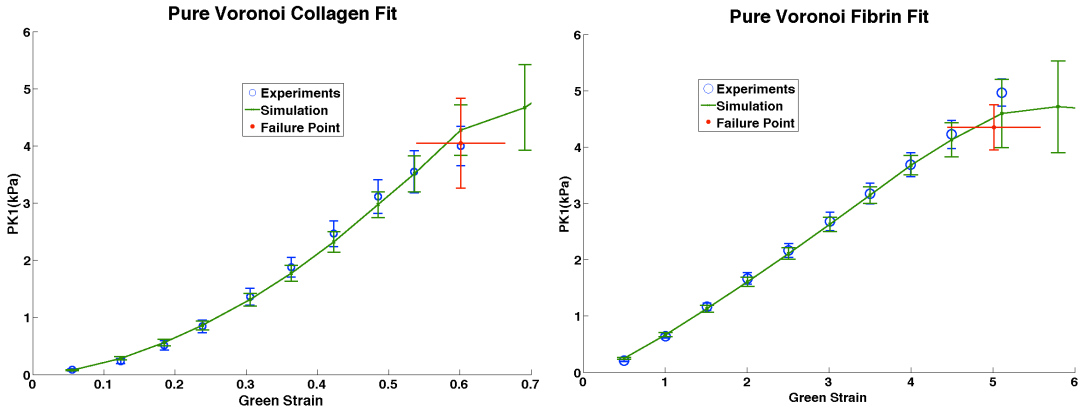

Figure 2a: Voronoi networks fit to pure collagen parameters. Unlike the Delaunay networks, the Voronoi networks are flexible enough to capture the mechanics of both the toe region and the linear region. The average failure strain and stress of the simulations in the fitting population match the values from the experiments.
Figure 2b: Voronoi networks fit to pure fibrin parameters. These Voronoi networks reproduce fibrin's failure stress and strain better than the Delaunay networks did.

2. Methods

2.1.A. General Network Generation

For either collagen or fibrin, a Voronoi network was generated to represent the microstructure. Networks were constructed containing around 600 fibers, connected at freely rotating joints. Since the Voronoi network has a degree of connectivity of four (meaning, on average, each node has about 4 connections to it), these networks are below the Maxwell limit (Maxwell, 1864) and thus unstable to small perturbations. Even so, such networks can be analyzed computationally, and the small-strain instability leads to a model giving the large toe region seen experimentally in uniaxial extension of collagen gels.

2.1.B. Model Mechanics

The mechanical behavior of each fiber in a given network was modeled using the exponential force-stretch relationship

$$F = \frac{A}{B}\exp\left(BE_f\right) - 1) \qquad (1)$$

where F is the force on the fiber, A is a composite parameter equal to the crossectional area of a fiber multiplied by the elastic modulus of a fiber at infinitesimal strain (Lake, Hadi, Lai, & Barocas, 2012), and B is a parameter describing the degree of nonlinearity. E_f, the Green strain of a fiber, was computed as

$$E_f = 0.5(\lambda_f^2 - 1) \qquad (2)$$

where λ_f is the fiber stretch. If a fiber exceeded a critical stretch λ_{crit} (different for each protein), it was deemed failed, and the prefactor A was reduced by a billion-fold for that fiber, making it mechanically insignificant without requiring a change to the network topology. This failure routine was easier to program and more computationally efficient than removing the fiber from the network matrices. Even though this is a fairly simple failure model, it has proven successful in describing the failure of collagen gels (Vanderheiden, Hadi, & Barocas, 2015). Following (Chandran & Barocas, 2007), the average Cauchy stress σ_{ij} for the network was calculated as follows:

$$\sigma_{ij} = \frac{1}{V} \sum_{\substack{boundary \\ nodes}} x_i F_j \qquad (3)$$

where V is the volume of the RVE being studied, x is the position of a boundary node, and F is the force on that node. The RVE was scaled according to protein content by the following equation:

$$Real\ Stress\ Factor = \sqrt{\frac{LA_f}{P_o}} \qquad (4)$$

where L is the total length of fibers, A_f is the cross-sectional area of an individual fiber, and P_o is the initial volume fraction of total protein. The Real Stress Factor relates the dimensionless microscale model calculations to macroscopic effects and units.

2.1.C. Fiber Properties

Table 1	Collagen	Fibrin
A (MPa*m^2)	24.24	2.88
B	3.0	0.6
λ_{crit}	1.41	3.40

Fiber model parameters (A, B, λ_{crit}) were regressed to pure-collagen and pure-fibrin data (see figure 2).

2.2. Co-Gel Network Models

We generated 50 networks of dimensions 2x2x2 using the Matlab voronoin function with about 575 random seed points. Proximity to the boundaries distorts network structure and behavior. Since we wanted to study the networks in an idealized setting, we clipped 1x1x1 boxes from the center of the 2x2x2 networks to eliminate edge effects. The network generation procedure is demonstrated, in simplified form, in figure 3.

These clippings yielded our pool of 50 distinct isotropic Voronoi network models, each containing approximately 680 fiber segments and 500 nodes.

These networks constituted a pool from which collagen and fibrin networks could be drawn for our future studies.

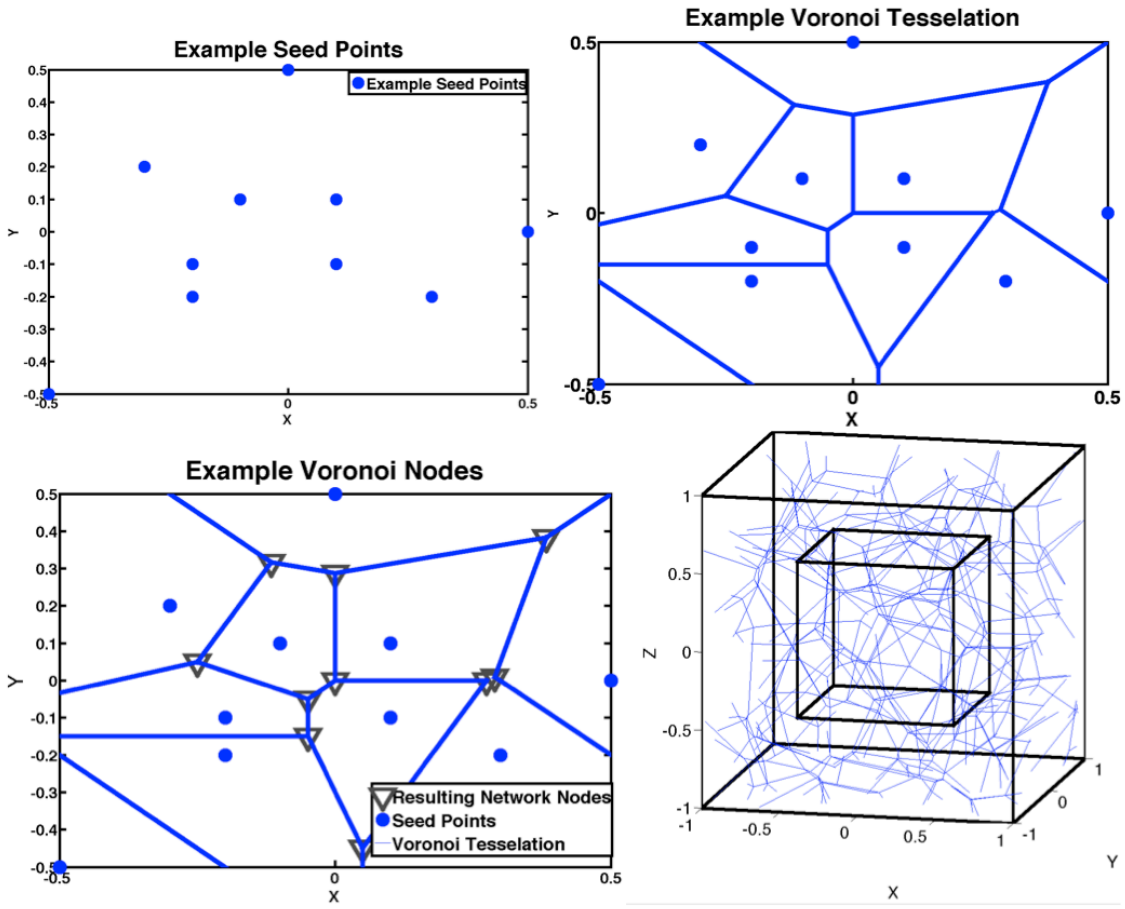

Fig 3: A-C demonstrate the procedure for generating a Voronoi network (2D example shown for clarity). In figure A, a 1x1 box is populated with seed points. In figure B, a Voronoi diagram is generated about those seed points. In figure C, the nodes and lines of the Voronoi diagram become the nodes and fibers of the network. The seed points are discarded. D illustrates the full sized network and clipping procedure (cube within a cube) structure used to make our pool of networks free of edge effects.

Interpenetrating networks were constructed by randomly selecting two different Voronoi networks from the pool, arbitrarily designating one as collagen and one as fibrin, and merging them. Then they were treated differently

depending on which model they were supposed to follow. In the cases which were supposed to be small networks within a larger network, the higher-density component was used unaltered, completely spanning the unit cube domain and thus representing a network that fully percolates the material space. For the lower-density component, however, the network was shrunk uniformly to a smaller size until the fiber density per unit volume of the whole representative volume element (RVE) was at the desired level. Thus, the lower-density network co-occupied a cubic "island" within the center of the RVE with the higher-density component, whereas the outer portion of the RVE contained only the higher-density component. The total unit size was scaled so that each RVE had the same total protein density. The parallel model networks were treated differently. The component networks in the parallel IPN had fibers randomly removed so that the total protein concentration was equal to that of a single unaltered network, and ratio of collagen to fibrin was as desired. For each island-case IPN, we generated one parallel IPN with the same ratio of collagen to fibrin. Example networks are shown in figure 4 with increasing minor box size.

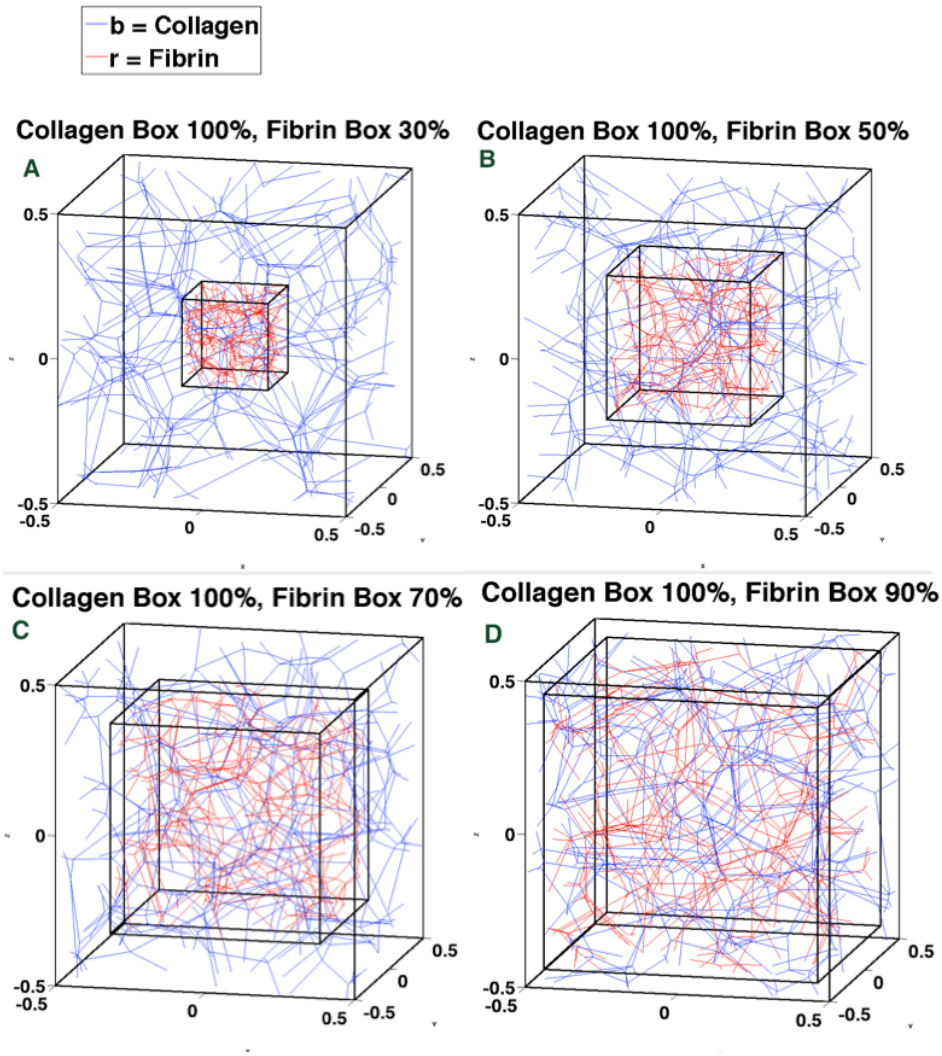

Figure 4: Island cases in order of increasing minor box size: 30% side length, 50% side length, 70% side length, and 90% side length. As minor box size increases, the collagen:fibrin ratio approaches 50:50, but never reaches it.

2.3. Simulated Extension and Network Interaction

Following our previous work (Lai, 2012), the simulated network was extended uniaxially by holding the –x face fixed and extending the network in the +x direction. The four transverse surfaces of the RVE were allowed to move inward as they were pulled by the interior fibers so as to have zero net force on

each surface, thus simulating traction-free boundaries. Interior nodes in the network were permitted to rearrange according to a Poisson's ratio of 0.4 so as to be at mechanical equilibrium (i.e., no net force on any interior node).

Prior work treated the two components of the IPN as completely separate entities which could not interact with each other. If the fibers collided, they were simply treated as occupying the same space without having any effect on each other. This ignored any effect caused by physical interaction between the two different networks. A novel feature of our model is that it allows interaction between the two networks. At each stretch step, a search was performed to identify any fibers that were within a critical distance of each other. In those cases, a new node was formed at the halfway point of the shortest line segment between the two fibers, and the intersecting fibers' paths were adjusted to snap to the new node. This node represents a point where the fibers stick together. Physically, this could be either a chemical crosslink or a point where the two fibers entangle. Since we did not know what the interacting distance between these two proteins should be, we used a conservative estimate of physical contact between the fibers ($d \leq 0.4\%$ of the RVE dimension, corresponding to just under the thickness of a fiber), assuming any unknown intermolecular attraction to be negligible. The interaction distance was set close to the diameter of a fiber to allow the fibers to come as near to each other as physically possible without passing through each other. Each of the intersecting fibers was thus converted into two new fibers. The new fibers were assigned rest lengths in proportion to

their current length such that the total rest length of the two new fibers was equal to the rest length of the original fiber. The fibers' strain history was preserved in this operation. Very small fibers (length≤ 0.01) were removed, and the two nodes at their ends were merged into one node at the fiber midpoint. This condensation was essential to keep the network size manageable and to avoid the computational difficulties associated with allowing extremely small fibers to populate the model. Our early studies without this step were plagued by exponential growth of clusters of mechanically insignificant fibers. These clusters would cause the simulations to freeze. Tests showed that the difference in macroscopic behavior produced by merging these nodes was negligible, so removing the small fibers to prevent clustering was an acceptable way to manage computational expense.

After the new connections between fibrin and collagen had been formed, any fibers strained beyond λ_{crit} were removed from the network by reducing the prefactor A in equation 1 by a factor of one billion to indicate that they had broken. This reduction eliminated the fiber's contribution to the network mechanics without forcing us to take the difficult step of updating the network topology. The new network was then allowed to equilibrate, and if any fibers were stretched beyond the critical stretch, the removal and re-equilibration steps were repeated until all fibers were in equilibrium and below the critical stretch (or the network failed). The re-equilibration loop was necessary to avoid jagged discontinuities in the stress-strain curve. Network failure was defined as the first

strain where the stress started to decrease; physically this corresponds to the strain where the co-gel starts to tear macroscopically. The network average stress was calculated using equation 3, and the process was repeated for the next stretch step.

2.4. Research Design

The stretching procedure was applied to co-gels ranging from 20% to 80% collagen, with the box sizes scaled so that the amount of total protein (collagen plus fibrin) was the same for each case. Below 50% collagen, fibrin occupies the major box and the island is made of collagen. This island model does not exist at 50%, because the networks would have to be set up in parallel (both networks spanning the box) instead of as an island embedded in a full network. Above 50% collagen, the roles of major and minor network are reversed, with collagen constituting the major box and fibrin making up the island. As stated earlier, pure component simulations were also run to determine the fiber model parameters. For each case, 5 different network realizations were constructed. Due to stochastic variation, this ended up creating island-case IPNs with a range of collagen:fibrin ratios. After creating these island cases, we generated parallel model IPNs with roughly the same collagen:fibrin ratios as the island cases and stretched them as well.

2.5. Verification of Model

To quantify the effect of the low-density component, we performed each

island network simulation with the low-density network removed (fiber interaction disabled). We compared the nodal displacement for each node in the higher-density network at 50% stretch in the simulations with the low density network present and the low density network absent. For each remaining node in the network, we calculated the final position at 50% stretch with and without the low-density network present, and then we averaged the absolute nodal displacement over all nodes. We compared those averages and found that the differences were minimal compared to the absolute displacements. We chose 50% stretch because beyond that ratio, fibers began to fail, making it impossible to compare active node displacement between the two simulation conditions.

2.6. Study Limitations:

The model is a model, not a true-to-life copy of physical co-gels. The co-gels were homogeneous mixtures of two proteins, not one block of one protein embedded in a larger block of a different protein. However, the simplified island model we have chosen is the easiest test case for series-like interaction between two distinct structures. In our model, fibrin and collagen have the same fiber diameter and the networks arise from Voronoi tessellation at all locations. However, we have seen in another study (Lai et al., 2012) that fibrin seems to become very wispy when it interacts with collagen, increasing the amount of crosslinking. We lack the required data to replicate this structure in our models, so must of necessity exclude it.

3. Results and Discussion

The double network topologies for a 79% collagen, 21% fibrin network are illustrated at four strain steps (0.25, 0.40, 0.69, 0.99) along with the corresponding stress-strain plot in figure 5. As the double network was stretched in the x direction, compression occurred in the y and z directions, resulting in entanglements between the outer majority component fibers and the inner island fibers. The failure strain is low, indicating that the stiffer collagen fibers dominated the behavior. While at first glance the fibrin seems to have decreased the failure stress somewhat, the effect is observed even when the fiber interaction mechanic is disabled. The lower observed stress is an artifact of the way we handled scaling, basing the real stress factor off the total amount of protein in the box. Since the composite networks have roughly the same protein density as the pure network, collagen effectively counts for less of the network space in the composite networks. This difference in density seems to account for most of the difference in observed stress, as there is little difference between the composite networks' stress-strain curves whether or not fibers from each network are allowed to interact with each other. Figure 6 shows what happened when the island cases' box size and real stress factors were replaced with those of the parallel network, confirming that the lower stress for the noninteracting island cases is largely due to scaling. Note also that the failure strain is still close to that of the pure collagen network despite the stresses being decreased.

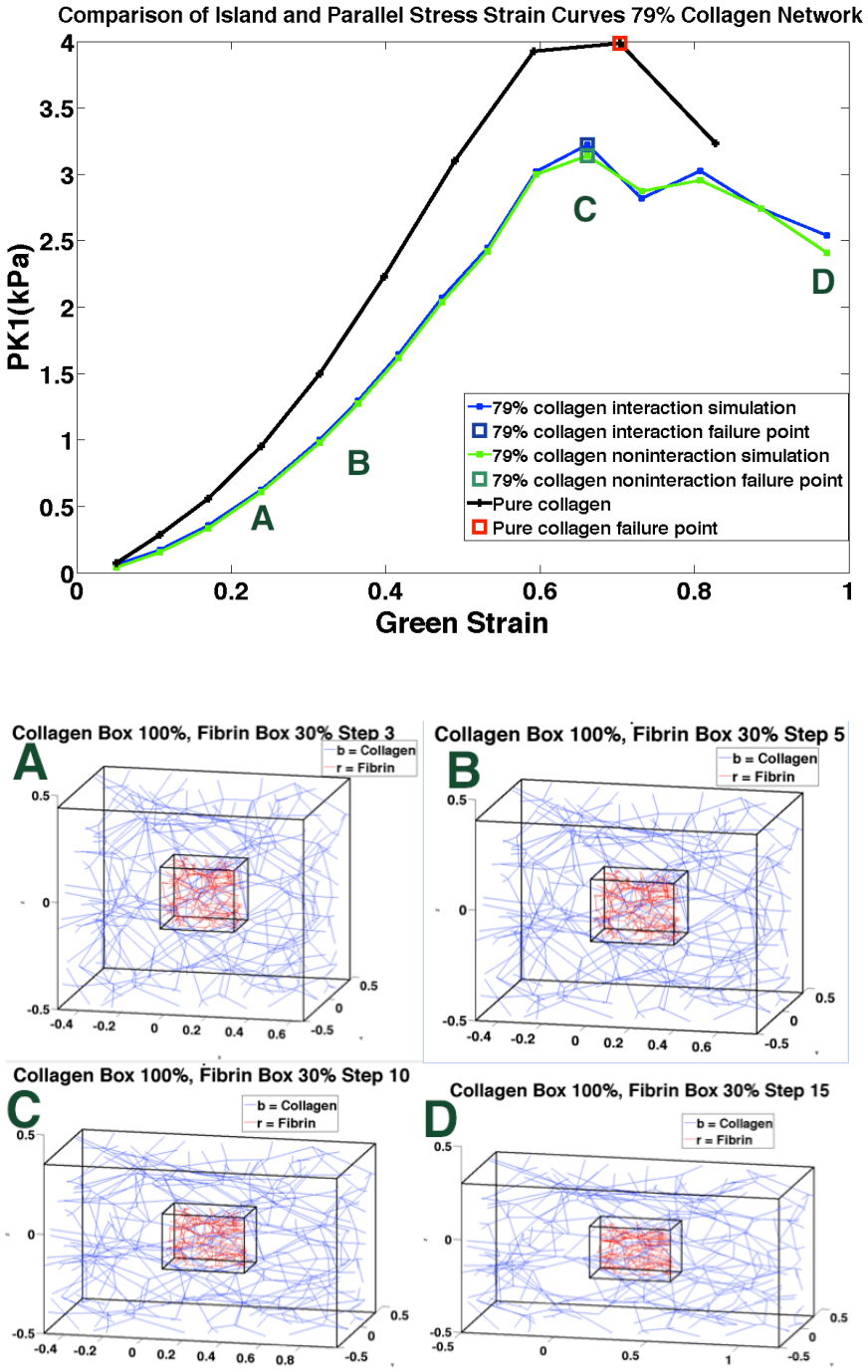

Figure 5: Example stress-strain curves with failure points marked, comparing a pure collagen network to a collagen network with a small embedded fibrin island, with snapshots of network geometry at various stretch steps pre and post failure.

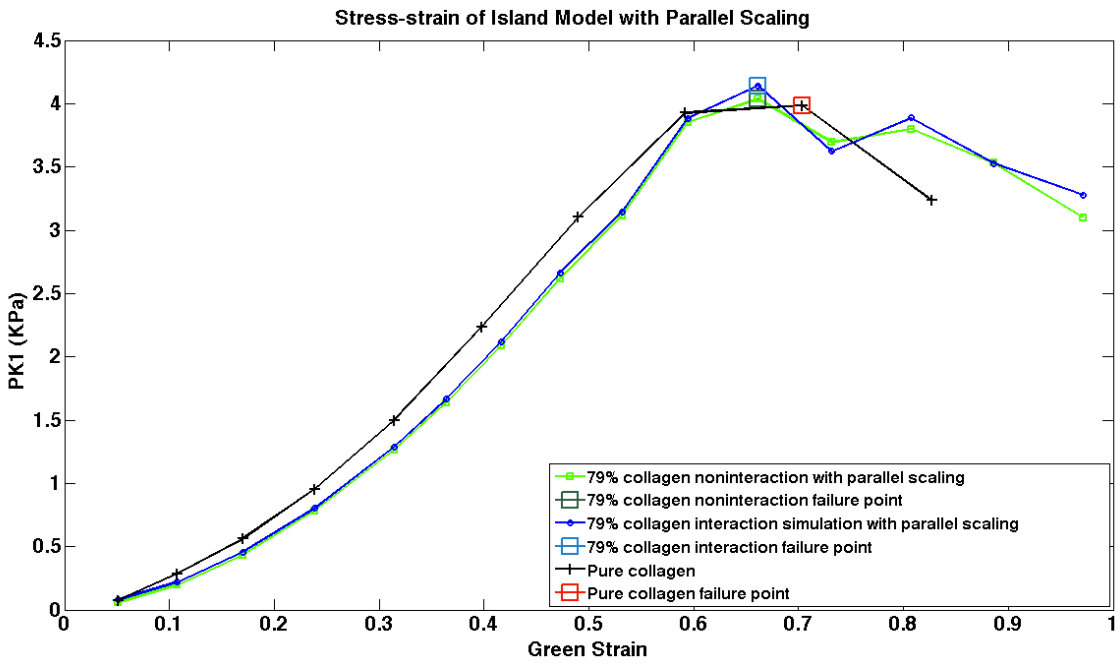

Figure 6: The same comparison as in Figure 5, but now the scaling factors are the same in the pure collagen and the island network. Substantial differences in failure stress disappear when the scaling factors are the same.

The hypothesis being tested in this study was that the experimentally observed transition from series to parallel behavior as collagen content increased as a result of the dominant protein transitioning from fibrin to collagen respectively, and that the minor component is contained within an embedded island network architecture that scales with concentration. We tested this by stretching full collagen networks with fibrin islands and the converse case at different volume fraction ratios. We expected to capture the experimentally observed transition in behavior with this model, but as figure 7 shows that was not the case.

When collagen is the minor protein, it has the largest effect in the parallel

model, and its effect begins at the lowest collagen concentration. As collagen volume fraction increases, the parallel model hovers around pure fibrin's failure strain until some threshold value of collagen is reached (around 30% by volume fraction). As the collagen volume fraction increases, collagen begins to exert a much stronger influence on the model, bringing the failure strain down closer to the experimentally observed values. From there on, the parallel model closely follows the experimental values.

In contrast, the interacting island model only begins exhibiting a difference from pure fibrin as the collagen:fibrin ratio approaches 1:1, and that difference is not as dramatic as in the parallel model. The noninteracting model's failure strain remains close to the failure strain of the dominant protein throughout the entire simulation, which is to be expected. In short, regardless of which protein constituted the major network, the major networks largely dominated the composite network's behavior. Combined island networks mostly behaved like the pure versions of their dominant networks. The interaction mechanic did have a minor effect on failure strain in fibrin-dominant networks, particularly for island networks with 40-49% collagen by volume, but the magnitude of interaction's effect was unexpectedly small.

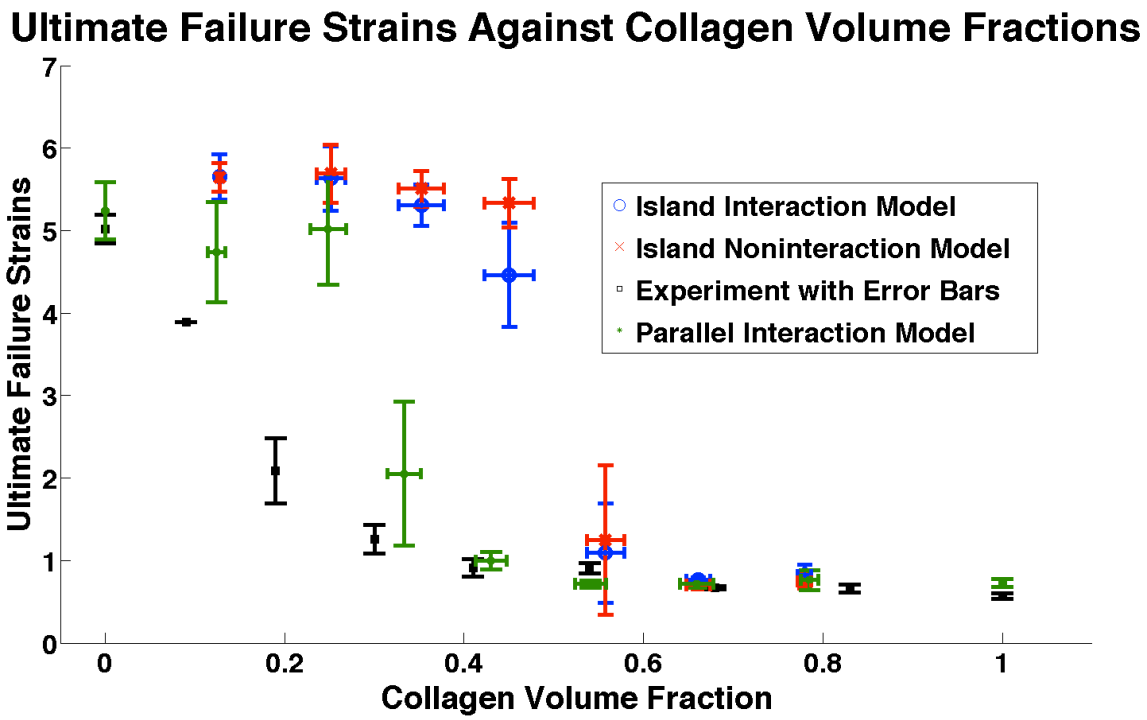

Figure 7: Ultimate failure strain vs. collagen volume fraction. When collagen's volume fraction <0.5, fibrin is the major protein and collagen forms the island. When collagen's volume fraction > 0.5, collagen is the major protein and the islands are made of fibrin. Here the effects of each model can be seen.

This discrepancy between our expectations and our results prompted us to verify that the model was performing correctly. First we looked at the average nodal displacements at 50% of failure strain with interaction turned on and turned off. According to our original hypothesis, turning on the interaction mechanic should have noticeably affected the average nodal displacements. However, as can be seen in figure 8, the nodal displacements exhibited almost no change due to the fibrin island's contribution and only a very small change due to the collagen island's contribution. The difference of average nodal displacements between the interaction condition and the noninteraction condition was smaller when

collagen occupied the larger box. Not only did the networks stretch less as the stiffer collagen exerted more of an influence on the double network, they also exhibited less variation in how much they stretched.

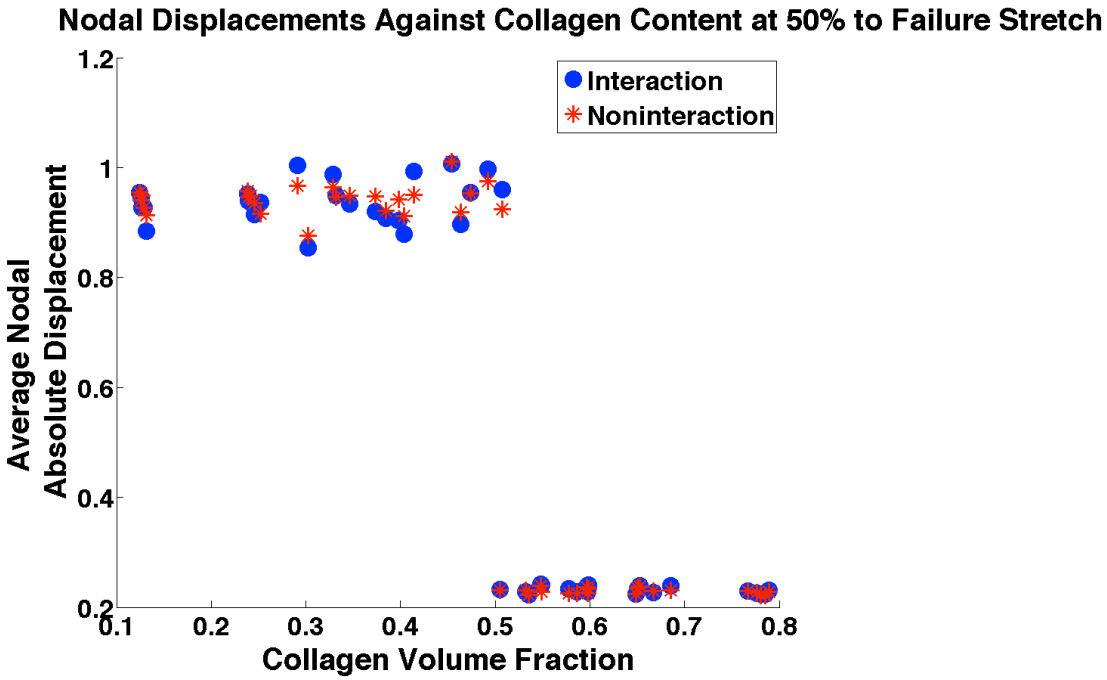

Figure 8: Comparison of average nodal displacement at 50% of failure strain against collagen content. The similarity in results between simulations with fiber interaction turned on and off indicates that fiber interaction was not as mechanically significant as expected.

These tests confirmed that the island networks were hardly affecting the mechanics at all, so we looked for a physical explanation. We considered the possibility that shrinking the minor network decreased the probability any given fiber would intersect with a fiber in the major network, meaning the two networks would not interact enough to cause mechanically significant entanglement. This would explain why there was no clear effect from the size of the minor network.

Indeed, figure 9a suggested that was the case because the average number of collagen-fibrin intersections in each network decreased as the embedded network's size decreased. However, when compared with the number of entanglements in the parallel model in figure 9b, there is little difference between the number of connections in the island model and the number of connections in the parallel model. Controlling for collagen volume fraction, there is no clear difference between the number of collagen-fibrin intersections of the island and the parallel cases, even when normalized to the total number of fibers in each network. Yet, despite the similar number of connections between the two component networks in the parallel and the island models, the mechanical behavior was noticeably different at a few key points. The collagen has a noticeable and significant impact on network failure strain around 30% volume fraction in the parallel model, as opposed to being fairly insignificant until it is the dominant protein in the island model. The difference in behavior despite having similar numbers of inter-network connections suggests that having collagen percolating the box has a more dramatic impact on behavior than simply having connections between the two networks. However, the difference between the island model's results with and without fiber-fiber interaction shows that fiber interaction does have some effect on behavior as well. The small magnitude of this effect might be due to the low number of fiber interactions.

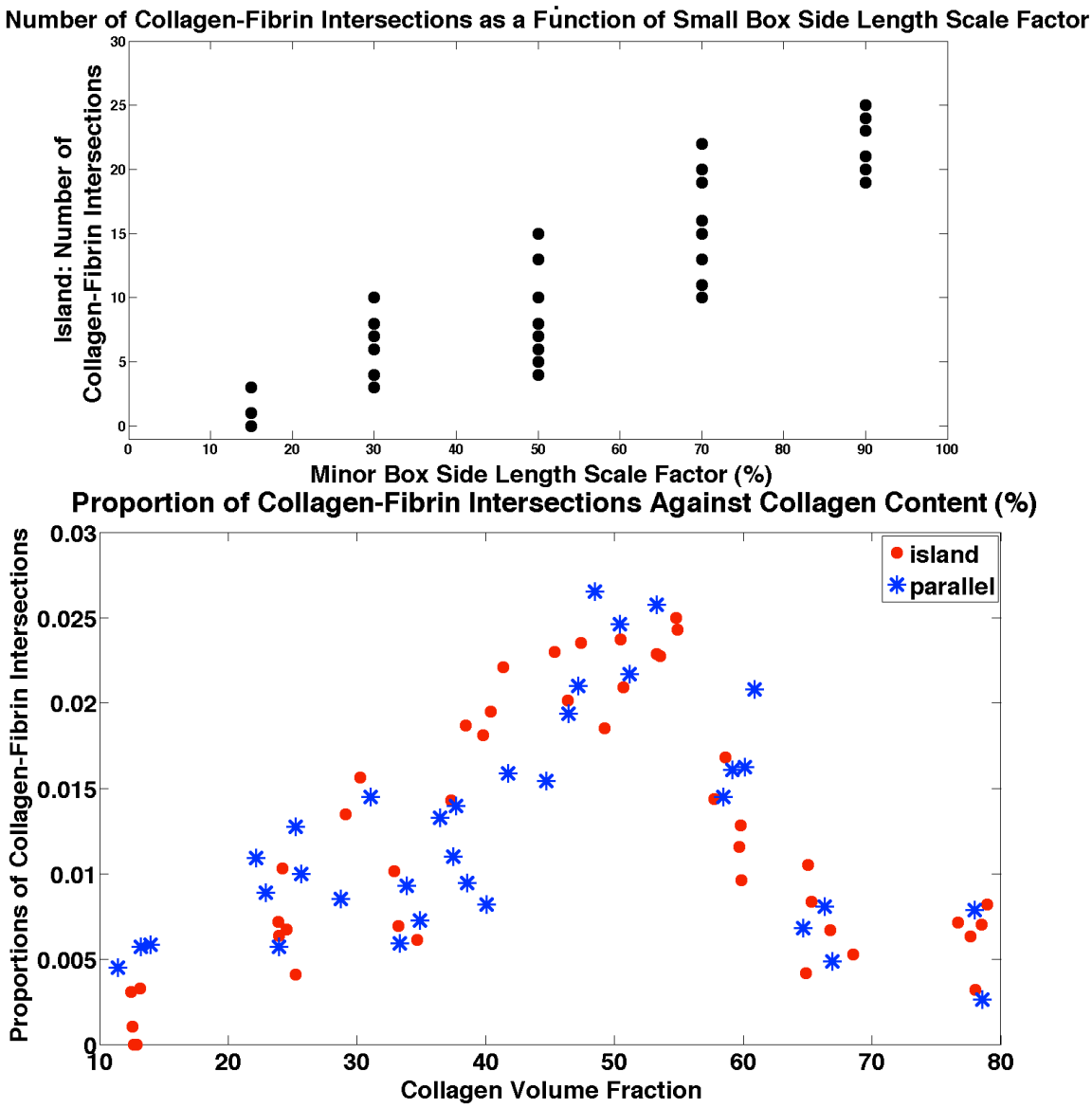

Figure 9a demonstrates the trend in the number of collagen-fibrin intersections increasing with box side length. This could provide a plausible explanation for why the collagen island has a greater effect on the major fiber network as its side length increases.
Figure 9b shows that the number and proportion of collagen-fibrin intersections as a function of collagen volume fraction is similar between the island and parallel models.

4. Conclusion and Future Work

Despite having similar numbers of fiber-fiber interactions at each collagen concentration, the island and parallel network behaved differently. In the parallel model, collagen was able to significantly influence the behavior of the network when it was the minor component, but only above a threshold which likely corresponds to the minimum concentration of protein needed to span the box. In contrast, the behavior in the island model was strictly dominated by the major protein component, with only a minor influence from interaction with the minor protein. Thus, it seems that while collagen-fibrin intersections have some effect on networks' mechanical behavior, the most significant factor determining network behavior is whether or not both networks span the box, and that an increase in collagen network percolation does not explain the transition from the series to the parallel model. If the networks both span the box, collagen will be able to affect behavior significantly. Otherwise, it will not. Regardless, the status of collagen's percolation is not enough to explain the experimental results.

The hypothesis that the observed transition from parallel to series behavior could be explained by a continuous network of the major component decorated with a nonpercolating interpenetrating network of the minor component is not supported by these simulations. However, this analysis does not mean that future studies should rely only a parallel model. Such a model would be unable to replicate mechanical properties of collage-deficient co-gels. In our old Delaunay simulations we observed that if the collagen network failed to percolate

in some cases and successfully percolated in others, the variance in stress was so high that the simulations were useless. This was much more likely to happen when one of the component networks had a low volume fraction. Since networks with low volume fractions had so few fibers to begin with, each fiber break contributed proportionally more toward destroying the network's path through the box. In the case of the networks in figure 10 some networks were even generated that didn't span the box from the start, resulting in large error bars.

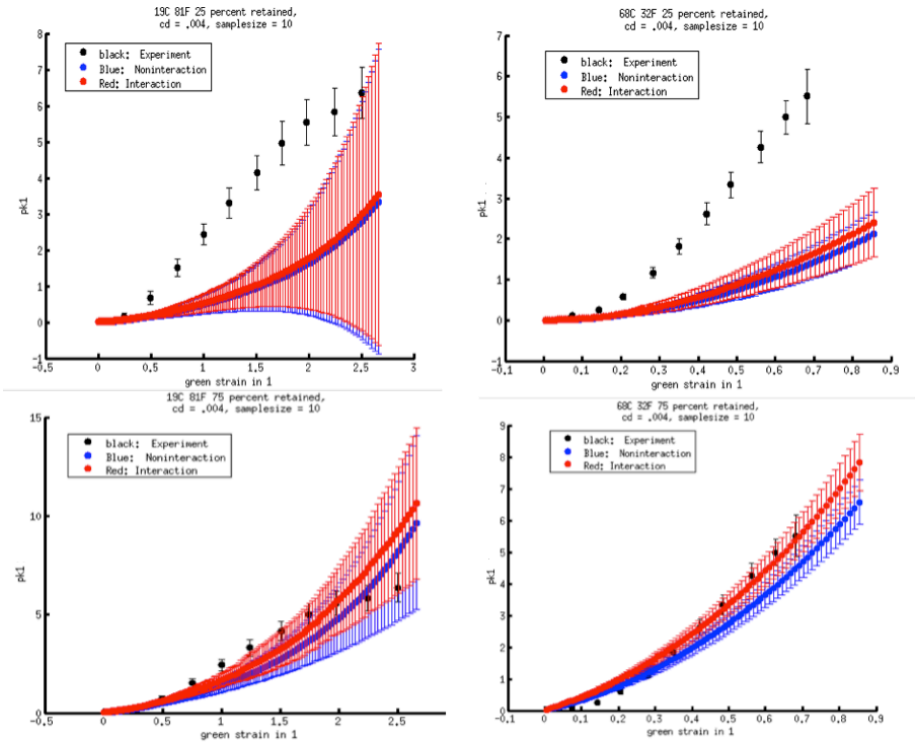

Figure 10: Illustration of the dramatic effect lack of network (specifically collagen) percolation can have on the stress-strain curve. These are from old Delaunay simulations, but the principle remains the same.

The most promising next step is to simply increase the allowable interaction distance and run the simulations again. Unlike the nonlinearity parameter, modulus, and λ_{crit} , the interaction distance is not a strictly physical parameter, and increasing it could remedy some deficiencies in our model. The cogel manufacture procedure means that collagen and fibrin have far more chances to intersect and bind to each other than our current IPN generation procedure allows. Our lab is currently working on this approach and has seen that increasing the interaction distance increases the number of collagen-fibrin intersections, in turn affecting the stress-strain curves.

Once a higher interaction parameter is fit, parallel and island simulations with and without interaction turned on could be run. This new suite of simulations would allow us to compare the impact of fiber interaction to network percolation. A parallel model with adequate fiber interaction might capture the behavior well, as it would behave as a series network at low collagen levels and as parallel networks at higher collagen levels.

Our preliminary tests have revealed that increasing the fiber interaction distance dramatically increases the computational expense of the model, so it will be very important to fit the interaction parameter correctly and efficiently on the first try, rather than simply running an automated recursive blind search. There might also be a risk that if the interaction distance is too large, the tiny fiber accumulation bug could return and the threshold size for fiber deletion would have to be increased in response. Lastly, the optimal fiber interaction distance

would probably vary depending on which model (parallel or island) was used to fit it, so it would be important to fit that parameter specifically for each model. Before fitting the interaction distance, it may be worthwhile to set the interaction distance to the maximum to see what the extreme case does to IPN behavior.

Bibliography

Chandran, P. L., & Barocas, V. H. (2007). Deterministic material-based averaging theory model of collagen gel micromechanics. *Journal of Biomechanical Engineering*, *129*(2), 137–147. https://doi.org/10.1115/1.2472369

Goulbourne, N. C. (2011). A constitutive model of polyacrylate interpenetrating polymer networks for dielectric elastomers. *International Journal of Solids and Structures*, *48*(7-8), 1085–1091. https://doi.org/10.1016/j.ijsolstr.2010.10.028

Hatami-Marbini, H., Shahsavari, A., & Picu, R. C. (2013). Multiscale modeling of semiflexible random fibrous structures. *CAD Computer Aided Design*, *45*(1), 77–83. https://doi.org/10.1016/j.cad.2011.10.002

Heris, H. K., Daoud, J., Sheibani, S., Vali, H., Tabrizian, M., & Mongeau, L. (2016). Investigation of the Viability, Adhesion, and Migration of Human Fibroblasts in a Hyaluronic Acid/Gelatin Microgel-Reinforced Composite Hydrogel for Vocal Fold Tissue Regeneration. *Advanced Healthcare Materials*, *5*(2), 255–265. https://doi.org/10.1002/adhm.201500370

Lai, V. K., Frey, C. R., Kerandi, A. M., Lake, S. P., Tranquillo, R. T., & Barocas, V. H. (2012). Microstructural and mechanical differences between digested collagen-fibrin co-gels and pure collagen and fibrin gels. *Acta Biomaterialia*, *8*(11), 4031–4042. https://doi.org/10.1016/j.actbio.2012.07.010

Lai, V. K. (2012). Mechanical Behavior of Collagen-Fibrin Co-Gels Reflects Transition From Series to Parallel Interactions With Increasing Collagen Content. *Journal of Biomechanical Engineering*, *134*(1), 011004. https://doi.org/10.1115/1.4005544

Lake, S. P., Hadi, M. F., Lai, V. K., & Barocas, V. H. (2012). Mechanics of a fiber network within a non-fibrillar matrix: Model and comparison with collagen-agarose co-gels. *Annals of Biomedical Engineering*, *40*(10), 2111–2121. https://doi.org/10.1007/s10439-012-0584-6

Maxwell, J. C. (1864). On the Calculation of the Equilibrium and Stiffness of Frames. *Philosophical Magazine*, *27*, 598–604.

Nachtrab, S., Kapfer, S. C., Arns, C. H., Madadi, M., Mecke, K., & Schröder-Turk, G. E. (2011). Morphology and linear-elastic moduli of random network solids. *Advanced Materials*, *23*(22-23), 2633–2637. https://doi.org/10.1002/adma.201004094

Raghavan, M. L., & Vorp, D. A. (2000). Toward a biomechanical tool to evaluate rupture potential of abdominal aortic aneurysm: Identification of a finite strain constitutive model and evaluation of its applicability. *Journal of Biomechanics*, *33*(4), 475–482. https://doi.org/10.1016/S0021-9290(99)00201-8

Rao, R. R., Peterson, A. W., Ceccarelli, J., Putnam, A. J., & Stegemann, J. P. (2012). Matrix composition regulates three-dimensional network formation by endothelial cells and mesenchymal stem cells in collagen/fibrin materials. *Angiogenesis*, *15*(2), 253–264. https://doi.org/10.1007/s10456-012-9257-1

Rowe, S. L., & Stegemann, J. P. (2006). Interpenetrating collagen-fibrin composite matrices with varying protein contents and ratios. *Biomacromolecules*, *7*(11), 2942–2948. https://doi.org/10.1021/bm0602233

Stylianopoulos, T., & Barocas, V. H. (2007). Volume-averaging theory for the study of the mechanics of collagen networks, *196*, 2981–2990. https://doi.org/10.1016/j.cma.2006.06.019

Vanderheiden, S. M., Hadi, M. F., & Barocas, V. H. (2015). Crack Propagation Versus Fiber Alignment in Collagen Gels: Experiments and Multiscale Simulation. *Journal of Biomechanical Engineering*, *137*(12), 121002. https://doi.org/10.1115/1.4031570

Veit, D., & T. I. (2012). *Simulation in Textile Technology - Theory and Applications*. Woodhead Publishing in Textiles. Retrieved from https://app.knovel.com/web/toc.v/cid:kpSTTTA00Q/viewerType:toc/root_slug:simulation-in-textile